HEALTH MONITORING OF WOVEN COMPOSITE STRUCTURES BY STRAIN FIELD METHODS: COMPARISON BETWEEN FIBRE BRAGG GRATING SENSORS ARRAYS AND DIGITAL IMAGE CORRELATION

Md Kharshiduzzaman[1,*], Andrea Bernasconi[2] and Lorenzo Comolli[3]

[1,*]Dipartimento di Meccanica, Politecnico di Milano,
Via La Masa 1, 20156 Milano, Italy
Email: md.kharshiduzzaman@polimi.it, web page: http://www.polimi.it

[2]Dipartimento di Meccanica, Politecnico di Milano,
Via La Masa 1, 20156 Milano, Italy
Email: andrea.bernasconi@polimi.it, web page: http://www.polimi.it

[3]Dipartimento di Meccanica, Politecnico di Milano,
Via La Masa 1, 20156 Milano, Italy
Email: lorenzo.comolli@polimi.it, web page: http://www.polimi.it

ABSTRACT

Fibre Bragg gratings (FBG) optical sensors can be easily attached on or embedded into composite laminates and used for the structural health monitoring of composites structures and of adhesively bonded joints. Therefore, the strain can be monitored by simply detecting the shift of the peak of reflected spectra of an array of FBG sensors. But problem arises when the strain fields along the gage length of FBG sensors are not uniform. In that case, the reflected spectra, which is the basis for strain estimation, does not produce a distinctive peak, rather, peak splitting occurs. Therefore, when peak splitting occurs, the strain values recorded by FBG sensors are not reliable. In this work, the response of FBG sensors for non-uniform strain field present in non-homogeneous material is investigated. The strain fields in woven composites are captured by two dimensional (2D) digital image correlation (DIC) technique. The spectral responses of FBGs and corresponding strain values are estimated by a Transfer-Matrix (T-Matrix) model in Matlab environment for different gage lengths of FBG sensors for DIC captured strain fields. It is seen that FBGs having smaller gage length produce sharp peaks of reflected spectra even when a large strain gradient exists, whereas peak splitting occurs for FBGs with higher gage lengths. Experiments were carried out for 3 different FBG gage lengths for verifications and the results were in good agreement with the numerically estimated observations by T-matrix simulations based on the strain fields obtained by DIC technique.

1   INTRODUCTION

In-service structural health monitoring (SHM) of engineering structures has become an important task in assessing their safety and integrity. High cost of maintenance, lack of precision in visual inspection and susceptibility of sensors to harsh environmental conditions has made structural health monitoring (SHM) mandatory. Among all other SHM techniques, strain-based methods are effective because the presence of damage in the structure under operational loads can alter the local strain distribution due to the load path changing within the structure. Both electrical resistance strain gages as well as fibre Bragg grating (FBG) optical sensors are usually used in the method to measure the strains. Due to the point nature of these sensors, strain monitoring is more suited to local structural 'hotspots' in large components rather than wide-area monitoring when individual or small no. of sensors are to be used. But thanks to the multiplexing capability of FBG sensors, multiple sensors can

be inserted into a single fibre thus forming an array of sensors that can be used to monitor much wider area [1, 2, 3].

FBG sensors provide a potential solution for strain based SHM techniques especially for composites and bonded structures. In composite materials, FBGs can be embedded inside the composite texture with a negligible effect on the mechanical properties [4, 5, 6, 7]. FBG strain sensors have been used in order to detect microscopic damages in composite laminates [8], for the investigation of delamination detection in CFRP laminates [9] as well as have been used to monitor crack growth in composite joints [10, 11]. For bonded composite joints, one of the most promising SHM techniques is backface (BF) strain technique. It is seen that, an array of FBG sensors can be very efficient [12] in capturing the BF profile which is vital for crack detection.

Even though FBG sensors possess numerous advantages, their spectral response when subjected to non-uniform strain distribution does not produce the distinctive peak which is needed for strain and temperature detection [8, 13, 14]. This is because in nonhomogeneous materials such as in woven composites, strain fields are much more complicated as high strain gradient exists. Therefore, the response of FBG sensors for non-homogeneous materials has to be investigated.

Huang et al. [15] developed Transfer Matrix (T-matrix) formalism to calculate the influence of different strain gradients on the reflective spectra of Bragg gratings. They proposed the use of a Bragg grating as a quasi-distributed strain sensor, based on T-Matrix, for the evaluation of the strain gradient present over the grating length. This technique, termed as 'Bragg Intra-Grating (BIG)' sensing could prove useful in applications where strain gradients exist and need to be monitored. Peters et al. [16, 17] later used this technique for experimental verifications and modified for high strain gradient applications [18].

In this work, the investigation of the response of FBG sensors due to non-uniform strain field present in non-homogeneous material such as in woven composite is discussed. Two dimensional (2D) Digital Image Correlation (DIC) technique is used to capture the strain field present in woven composites and that strain field is then used in T-Matrix to simulate FBG response. After that, experiments were carried out using FBGs to compare the results for different gage lengths.

2 INVESTIGATION PROCEDURE

2.1 Specimen

Composite strip made of 2x2 plain weave carbon fabric was used in this investigation. The detailed dimensions of the strips are shown in Fig. 1.
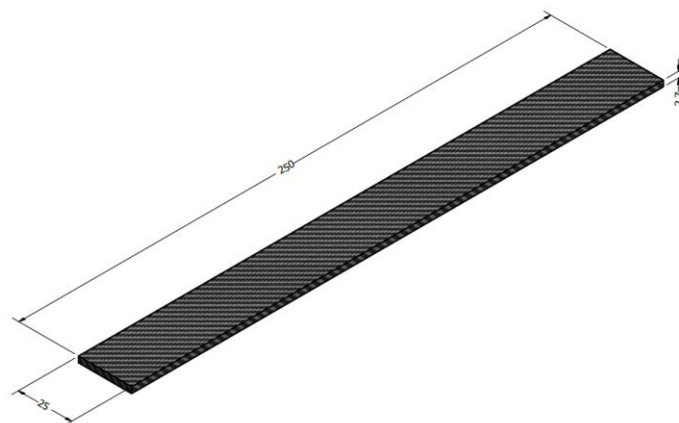

Figure 1: Woven composite strip. (All dimensions are in mm)

2.2 2D Digital image correlation

At first the specimens were cleaned with Acetone in order to remove dust. The region on which random speckle pattern will be created was marked by applying adhesive tape at the end of both sides

of the specimen. Then white paint was applied within the portion of the specimens cleaned before and was allowed to dry. The speckle was created by spraying black paint from an airbrush.

A DSLR camera (CANON EOS 400D, Tokyo, Japan) with a 100 mm macro lens was used to capture digital images. A tripod was used to fix the camera in such a position that the specimen surface remains in the same plane parallel to the image sensor. A white light source was used to illuminate the specimen and was not moved during the load application and image acquisition of the deformed specimen so that, all the images could have taken under same constant illumination. The machine that applied the loads is a servo-hydraulic system MTS Landmark™ Testing Solutions, USA with a capacity of 100 kN. The reference image was captured at 0 kN. Then, images of deformed specimen starting from 1 kN till 8 kN were captured with a step of 1 kN. All the acquired images were selected at 3888x2592 pixel resolution. The system was calibrated considering a scale factor value equal to 80 pixels/mm. Processing of the acquired images was done by Vic-2D software from Correlated Solutions, Inc., USA to obtain the strain information.
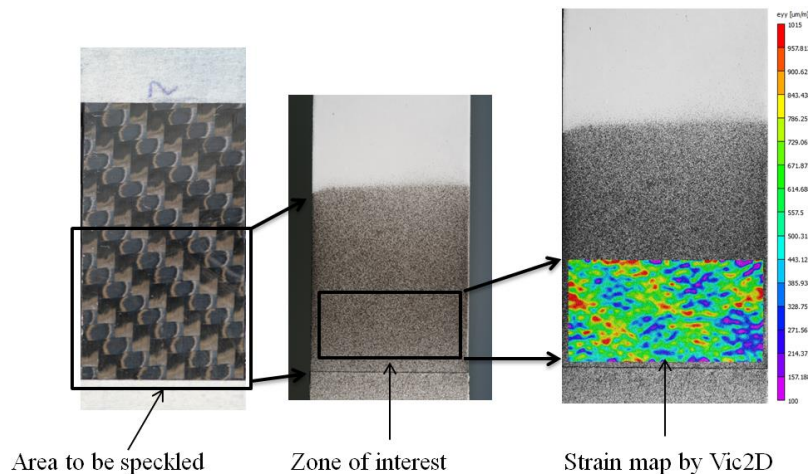

Figure 2: Strain mapping for woven composite using Vic-2D.

Vic-2D software assigns a mesh of "subsets" or windows across the Region Of Interest (ROI) and finds a unique point for each subset for correlation. The step size is the pixel number the software uses to track subsets, e.g. for a step size of 5 pixels, the software tracks the subset area for every 5 pixels. Subset size was selected 29 (a 29x29 pixel window) with 5 pixels step size. A demonstration of the strain mapping using Vic-2D is shown in Fig. 2 for 2 kN load level.

Once the strain field was mapped, strain profiles were extracted along the unit cell for different load levels across the two paths (White and Red) as shown in Fig. 3.
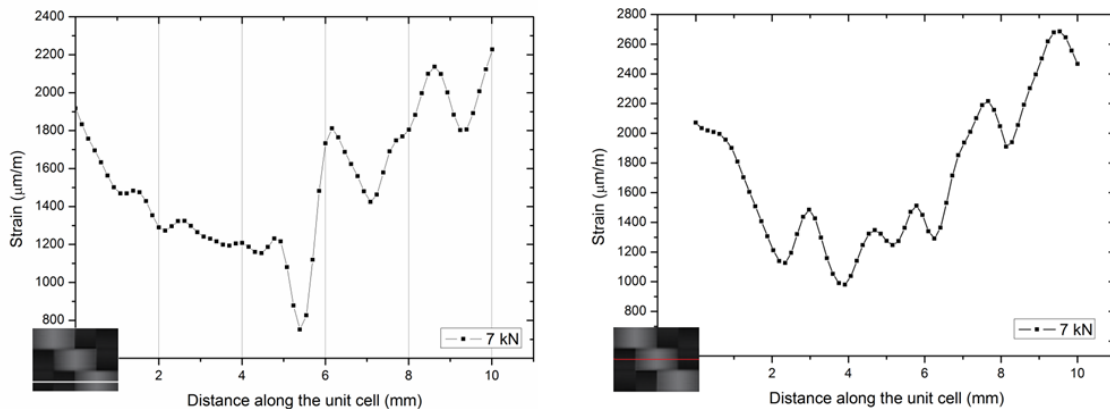

Figure 3: Strain profile along the unit cell for two different paths from DIC strain map (for this case- 7 kN load)

Strain profiles were extracted along two different paths in order to facilitate the installation of different gaged FBGs within the same unit cell later in the experiments.

2.3 T-Matrix simulation

The numerical model used to simulate the reflected spectra of a FBG sensor that is subjected to an arbitrary strain profile is based on the transfer matrix (T-matrix) model [15, 19, 20, 21]. This matrix approach is capable to discretize a single grating into a series of separate gratings each having reduced overall lengths and different grating lengths, and describing each with its own T-matrix. After that, by combining all the matrices, the properties of the initial non-uniform grating can be achieved, and the reflection spectrum of FBG sensor can be obtained for that given strain profile.

So, it is clear that, if the strain profile is known, the reflected spectrum of FBG sensor for that strain profile can be estimated by T-matrix model.
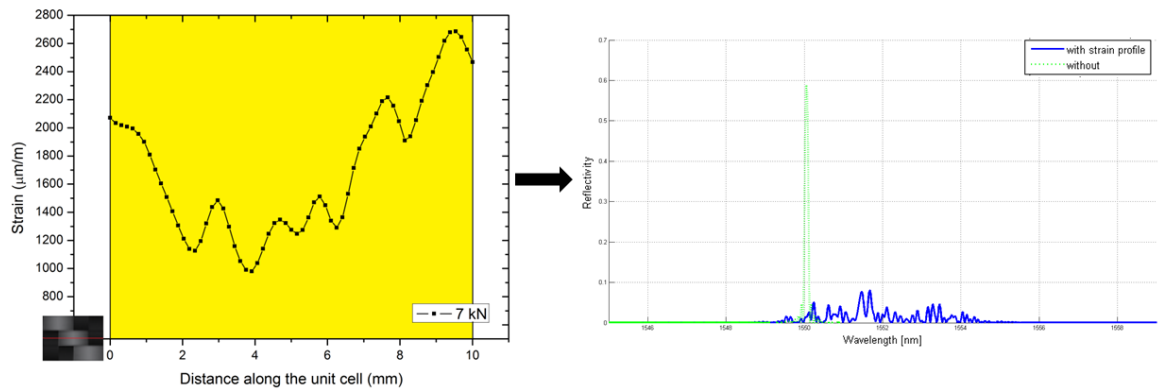

Figure 4: Left- Strain profile sensed across the gage length of 10 mm FBG is highlighted by yellow zone; Right- T-Matrix simulated spectrum for sensed strain profile and compared with the spectrum for no strain (for 7 kN load level).

At first, reflected spectra and corresponding strain values were obtained for all load levels for 10 mm FBG by using DIC measured strain profiles along the red path into T-matrix method. Fig. 4 (Right) shows simulated reflected spectra for 7 kN load level and compared with the reflected spectra when no strain is applied which is denoted as 'without' in the figure. It can be seen that, the response from a 10 mm FBG sensor for non-uniform strain profile does not provide a distinctive peak, and peak splitting occurs. The peak of the reflected spectrum from FBG sensor is the main feature to measure strain and therefore, when there is no distinctive peak, the strain measurement becomes inaccurate.
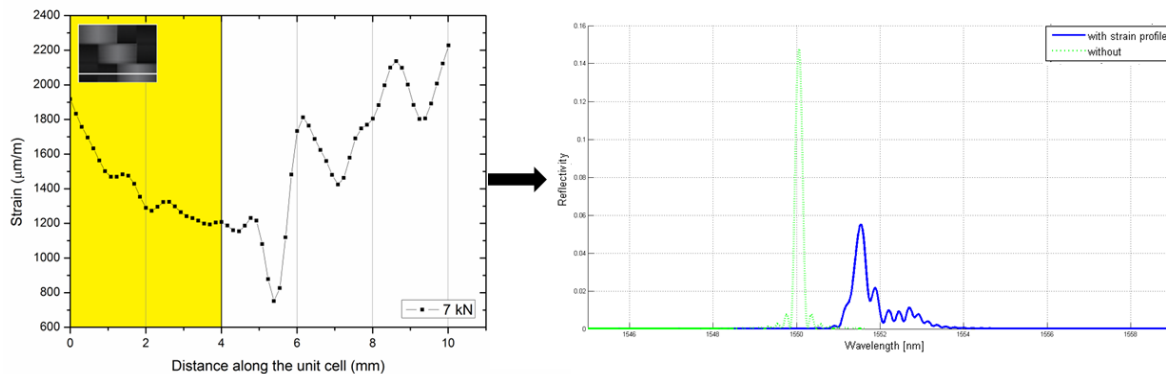

Figure 5: Left- Strain profile sensed across the gage length of 4 mm FBG is highlighted by yellow zone; Right- T-Matrix simulated spectrum for sensed strain profile and compared with the spectrum for no strain (for 7 kN load level).

Next, 4 mm FBG gage length was selected. As the gage length of the FBG is less than the length of the unit cell, T-matrix simulations were performed for strain profile segments from 0 mm to 4 mm and the strain profile along the white path was selected in this case. Simulation was carried out for all load levels.

Fig. 5 shows the reflected spectra of 4 mm FBG sensor for non-uniform strain profile segment from 0 mm to 4 mm for 7 kN load level and compared with the reflected spectra when no strain is applied. We can observe that the spectral response of a 4 mm FBG retains the main characteristic needed for strain estimation, i.e. the peak. Small chirping effect is also present, but not as dominant as the 10 mm case to cause the peak to split. Therefore, from these observations, it is clear that, by reducing the gauge length peak splitting can be avoided.
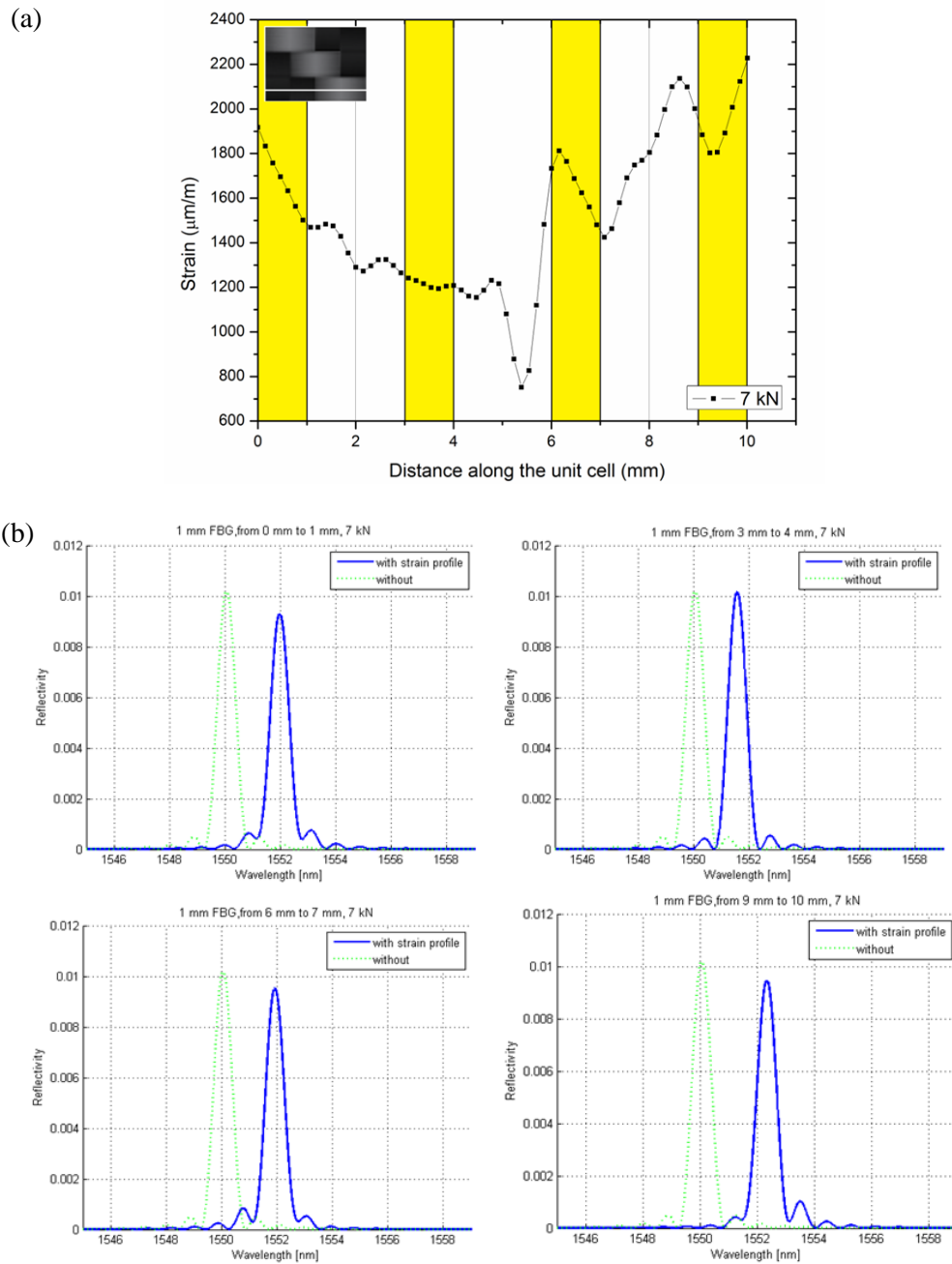
(a)

(b)

Figure 6: (a) Strain profile segments sensed across the 1 mm gage length of an array of four FBGs are highlighted by yellow zones; (b) T-Matrix simulated spectra for sensed strain profile segments for all positions (7 kN load level) and compared with the spectra for no strain.

Finally, 1 mm FBG gage length was selected to simulate the reflected spectrum by T-matrix method. In this case also, the strain profile along the white path was selected. Reflected spectra were simulated for 4 different positions within the unit cell. This is because, instead of having the response of single 1 mm FBG sensor, we wanted to simulate the response for an array of 4 FBGs having 1 mm gage length.

Fig. 6 shows the spectral response of 1 mm FBG sensor for four different positions within the strain profile along the unit cell's white path. It can be seen that, for all the positions, reflected spectra from 1 mm FBG produces a distinctive peak and peak splitting phenomenon is completely eliminated which makes this gage length very much suitable for high strain gradient applications such as in woven composites. However, this also implies that values are read over small regions, resulting into local values which may differ from average ones.

3   EXPERIMENTAL

FBG sensors having three gage lengths, 10 mm, 4 mm and 1 mm were installed in two 2x2 plain weave woven composite specimens having dimensions same as described in Fig. 1. FBG sensor having 10 mm and 4 mm gage length were single sensors and bonded on one specimen whereas for 1 mm FBG sensor, an array of 4 sensors were installed in another specimen. The installation positions for all the sensors correspond to their respective positions and paths within the unit cell for which T-matrix simulated reflected spectra were performed using DIC captured strain profiles.
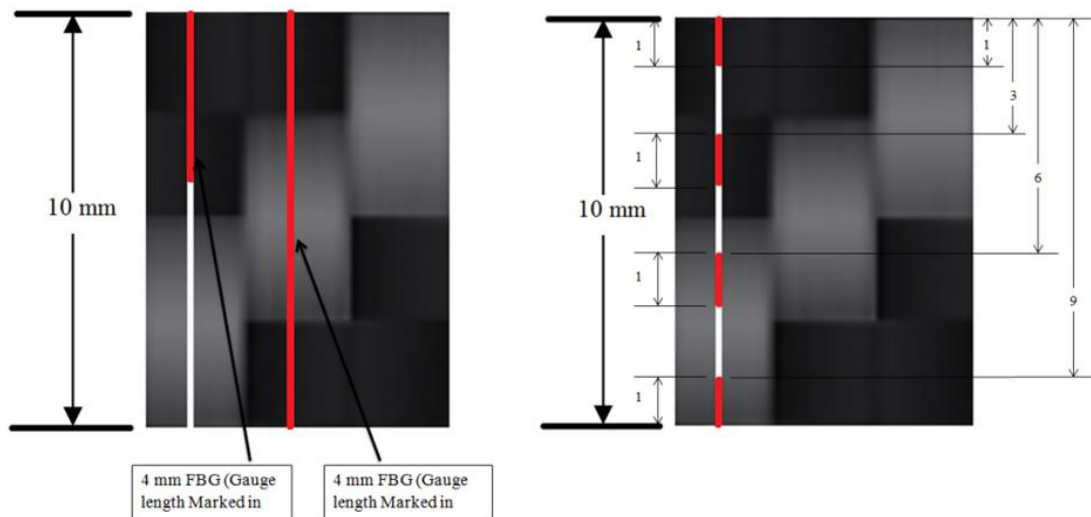

Figure 7: Installation configuration of FBG sensors within a single unit cell of 2x2 plain weave woven carbon fibre composite ; Left- single 4 mm and 10 mm FBG sensors installation positions, right- An array of four 1 mm FBG sensors.

Experimental investigation was carried out in a servo-hydraulic system MTS Landmark™ Testing Solutions, USA with a capacity of 100 kN. The conditionings of the FBG sensors were done by Hottinger Baldwin Messtechnik GmbH (HBM) DI410 having 1000 Hz acquisition capacity with four optical sensor channels. Static loads were applied to both specimens starting from 1 kN to 8 kN with a step of 1 kN.

4   RESULTS AND DISCUSSION

4.1 10 mm FBG sensor

The comparison between the experimental and simulated results for 10 mm FBG sensor is shown in Fig. 8.
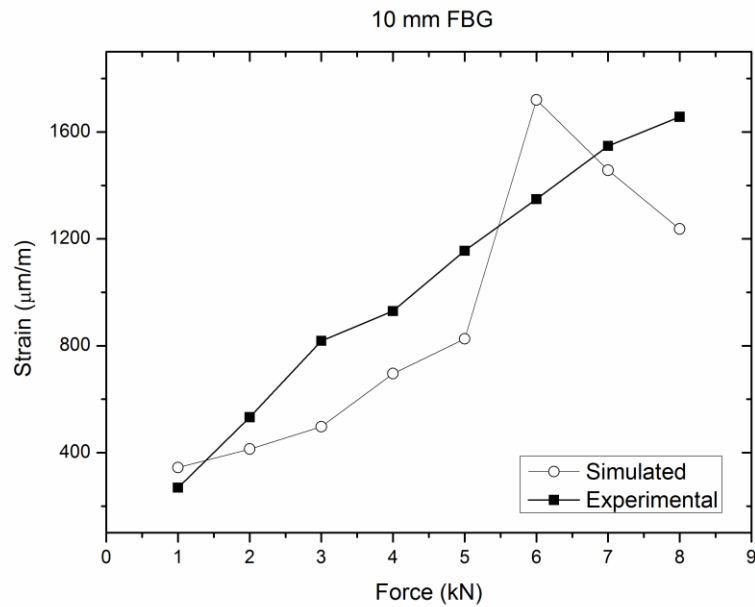
Figure 8: Comparison between simulated and experimental results for 10 mm FBG.

What can be observed from Fig. 8 is that the results are not in agreement at all. Due to the presence of strain gradients, chirping of grating is likely to have occurred, leading to peak splitting as seen in T-matrix simulations for 10 mm FBG sensor earlier. Due to this chirping effect, as no distinctive peak was not produced by the reflected spectrum of FBG, therefore the strain readings are also not reliable.
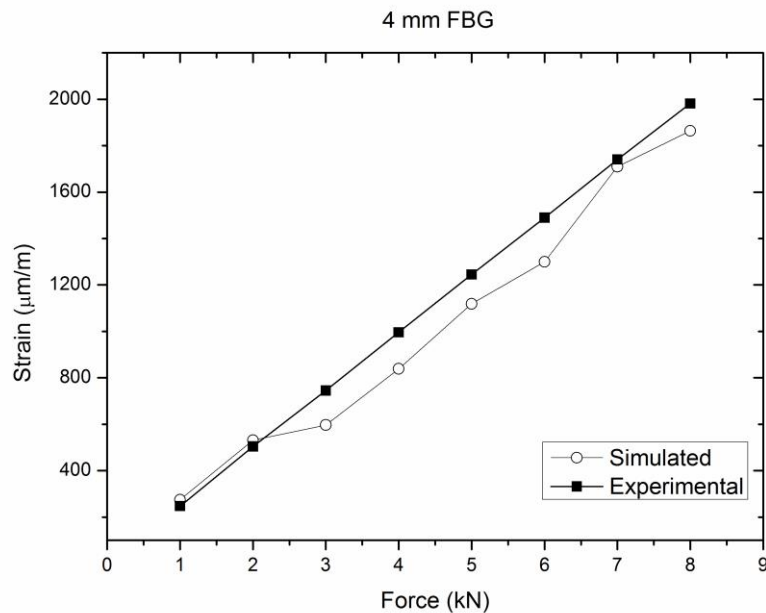
4.2   4 mm FBG sensor

Figure 9: Comparison between simulated and experimental results for 4 mm FBG.

The comparison between the experimental and simulated results for 4 mm FBG sensor is shown in Fig. 9. We can see that, the experimental results are in agreement with the T-matrix simulated results

using the strain profiles obtained from DIC technique. The simulated results from 3 kN till 6 kN shows a small constant deviation from the experimental results may be due to slipping of the specimen inside the grips during DIC experiment at 3 kN. But if we carefully observe the slope from 3 kN to 6 kN, it is almost the same as the experimental one.

As seen from the previously shown T-matrix simulation for 4 mm FBG sensors, they do not undergo grating chirping as of 10 mm FBGs. Therefore peak splitting is not dominant for 4 mm FBGs which results into sharp peaks in their reflected spectra. Hence, they are suitable for strain gradient applications such as in woven composites.
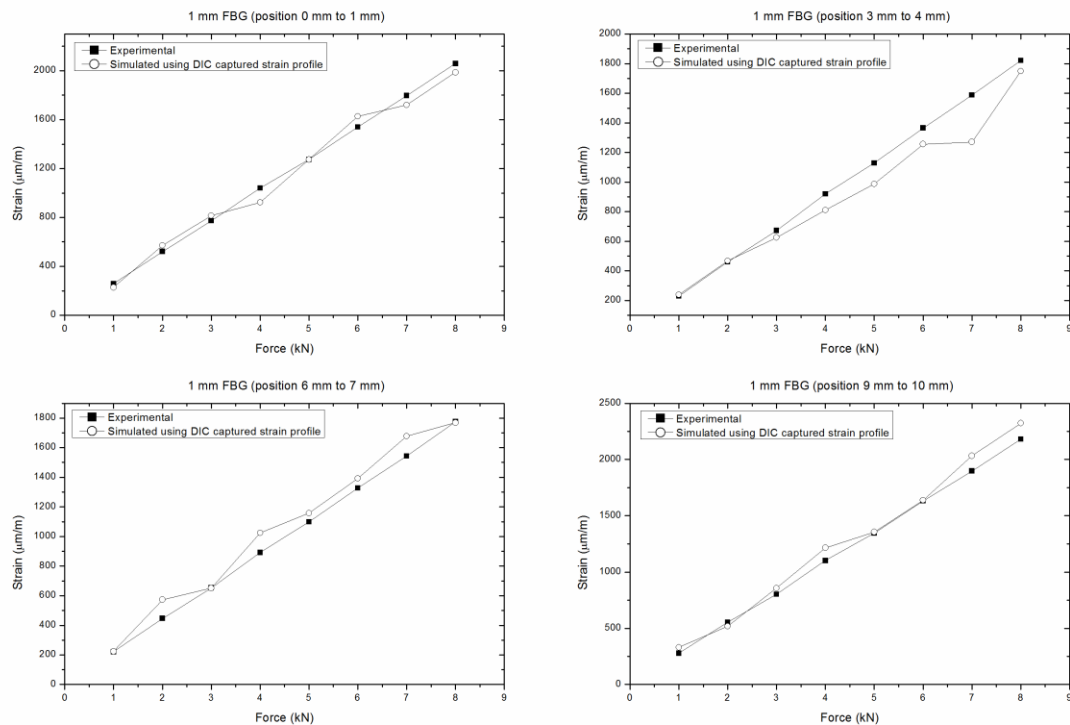
4.3 1 mm FBG sensor

Figure 10: Comparison between the experimental and simulated results for 1 mm FBG sensors array.

From Fig. 10 it can be seen that for all four positions, the 1 mm FBG sensors of an array, apart from one single deviated simulated result for 7 kN at position 3 mm – 4 mm, produce excellent agreement between the experimental and T-matrix simulated results using DIC captured strain profile segments for corresponding sensor positions. The single deviation at position 3 mm- 4 mm at 7 kN load level may be due to the fact that, the strain profile segment for this position at that load level obtained by poor DIC correlation due to poor local speckle characteristics for that particular position.

As seen from the T-matrix simulations for 1 mm FBGs before, the chirping effect was completely eliminated for this case and, therefore FBGs produce distinctive peak in their reflected spectra. Hence, they are ideal for strain gradient applications and can produce strain measurement with high accuracy.

One critical observation from the Fig. 10 is that, depending on their position within the unit cell, strain values sensed by the FBGs changed as well. For example, for 0 mm to 1 mm position, the strain value sensed by the FBG at 8 kN is about 2000 μm/m whereas at 6 mm to 7 mm position, it sensed strain value around 1750 μm/m for 8 kN load level. Therefore, the strains recorded by these small FBGs are local strain values which can differ from overall global strain scenario. In order to

compensate this effect while capturing strain profile, an array containing large number of these small FBG sensors can be implemented by placing them closer to each other.

5   CONCLUSIONS

The spectral response of FBG sensors having different gauge lengths for strain fields having high strain gradient had been studied in this work. It is seen that, spectral response of 10 mm FBGs does not perform well in non-uniform fields. This is because they fail to produce distinguishable single peak which is a must for measuring strain. On the other hand, 4 mm FBG's reflected spectrum produce a single peak even though small chirping effect is present.

Finally, it is observed that, reflected spectra from 1 mm FBG sensor produce not only a distinctive peak but also the chirping effect is completely eliminated in this case thus making this configuration very much suitable for high strain gradient applications such as in woven composites. However, due to their small size, they produce local strain readings that may differ from global strain readings.

REFERENCES

[1]   A. Bernasconi, M. Carboni, L. Comolli. Monitoring of fatigue crack growth in composite adhesively bonded joints using Fiber Bragg Gratings. *Procedia Engineering*, **10**, 2011, pp. 207–212.

[2]   A. Bernasconi, L. Comolli. An investigation of the crack propagation in a carbon-fiber bonded joint using backface strain measurements with FBG sensors. *Proceedings of the 22nd International Conference on Optical Fiber Sensors*, *Beijing, China, October 15-19, 2012,* Proc. SPIE. 8421, 2012, 84214Y.

[3]   M. Haq, A. Khomenko, L. Udpa, S. Udpa. *Fiber Bragg-Grating Sensor Array for Health Monitoring of Bonded Composite Lap-Joints*. Experimental Mechanics of Composite, Hybrid, and Multifunctional Materials. Springer International Publishing. Vol 6, Chap 22, pp. 189- 195.

[4]   I. Herszberg, H.C.H. Li, F. Dharmawan, A.P. Mouritz, M. Nguyen, J. Bayandor. Damage assessment and monitoring of composite ship joints. *Composite Structures*, **67 (2)**, 2005, pp. 205–216.

[5]   H.C.H. Li, I. Herszberg, C.E. Davis, A.P. Mouritz, S.C. Galea. Health monitoring of marine composite structural joints using fibre optic sensors. *Composite Structures*, **75**, 2006, pp. 321-327.

[6]   R.A. Silva-Muñoz, R.A. Lopez-Anido. Structural health monitoring of marine composite structural joints using embedded fiber Bragg strain sensors. *Composite Structures*, **89**, 2009, pp. 224–234.

[7]   A. Papantoniou, G. Rigas, N.D. Alexopoulos. Assessment of the strain monitoring reliability of fiber Bragg grating sensor (FBGs) in advanced composite structures. *Composite Structures*, **93**, 2011, pp. 2163–2172.

[8]   Y. Okabe, T. Mizutani, S. Yashiro, N. Takeda. Detection of microscopic damages in composite laminates with embedded small-diameter fiber Bragg grating sensors. *Composites Science and Technology*, **62**, 2002, pp. 951–958.

[9]   S. Takeda, Y. Okabe, N. Takeda. Delamination detection in CFRP laminates with embedded small-diameter fibre Bragg grating sensors. *Composites: Part A*, **33**, 2002, pp. 971–980.

[10] R. Jones, S. Galea. Health monitoring of composite repairs and joints using optical fibers. *Composite Structures*, **58**, 2002, pp. 397-403.

[11] J. Palaniappan, S.L. Ogin, A.M. Thorne, G.T. Reed, A.D. Crocombe, T.F. Capell, S.C. Tjin, L. Mohanty. Disbond growth detection in composite–composite single-lap joints using chirped FBG sensors. *Composites Science and Technology,* **68**, 2008, pp. 2410-2417.

[12] A. Bernasconi, M. Kharshiduzzaman, L.F. Anodio, M. Bordegoni, G.M. Re, F. Braghin, L. Comolli. Development of a monitoring system for crack growth in bonded single-lap joints based on the strain field and visualization by augmented reality. *The journal of adhesion*, **90**, 2014, pp. 496-510.

[13] S. Daggumati, E. Voet, W. Van Paepegem, J. Degrieck, I. Verpoest. Local strain in a 5-harness satin weave composite under static tension: Part I – Experimental analysis. *Composites Science and Technology,* **71**, 2011, pp. 1171–1179.

[14] D.H. Kang, S.O. Park, C.S. Hong, C.G. Kim. The signal characteristics of reflected spectra of fiber Bragg grating sensors with strain gradients and grating lengths. *NDT & E International*, **38**, 2005, pp. 712–718.

[15] S. Huang, M. Ohn, R. Measures. Phase-based bragg intragrating distributed strain sensor. *Applied Optics*, **35**, 1996, pp. 1135–1142.

[16] K. Peters, M. Studer, J. Botsis, A. Iocco, H. Limberger, R. Salathé. Embedded optical fiber Bragg grating sensor in a nonuniform strain field: Measurements and simulations. *Experimental Mechanics*, **41**, 2001, pp. 19–28.

[17] K. Peters, P. Pattis, J. Botsis, P. Giaccari. Experimental verification of response of embedded optical fiber Bragg grating sensors in non-homogeneous strain fields. *Optics and Lasers in Engineering*, **33**, 2000, pp. 107-19.

[18] M. Prabhugoud, K. Peters. Modified transfer matrix formulation for Bragg grating strain sensors. *Journal of lightwave technology*, **22**, 2004, pp. 2302-2309.

[19] A. Othonos. Fiber Bragg gratings. *Review of Science Instrument*. **68**, 1997, pp. 4309-4341.

[20] Z. Kaczmarek, A. Sikora, Influence of a uniform fiber Bragg grating on the accuracy of measuring an impulsive strain. *Optica Applicata* , **XXXVIII (2)**, 2008, pp. 305-314.

[21] H.Y. Ling, K.T. Lau, W. Jin, K.-C. Chan. Characterization of dynamic strain measurement using reflection spectrum from a fiber Bragg grating. *Optics Communications*, **270 (1)**, 2007, pp. 25–30.